

Gyromagnetic factors of the high-spin yrast states in some doubly even germanium and selenium isotopes

P. K. Rath

Department of Physics, Indian Institute of Technology Kanpur, Kanpur-20 80 16, India

S. K. Sharma*

Institut für Theoretische Kernphysik der Universität Bonn, D-5300 Bonn, West Germany

(Received 2 June 1988)

The gyromagnetic factors associated with the yrast levels (with $2^+ \leq J^\pi \leq 12^+$) in some doubly even Ge and Se isotopes are discussed in a microscopic, parameter-free perspective in terms of the variational wave functions resulting from realistic effective interactions operating in the $(2p_{3/2}, 2p_{1/2}, 1f_{5/2}, 1g_{9/2})^{\pi,\nu}$ configuration space. The estimates for the g factors of the yrast 2^+ states are consistent with the available experimental results. The calculations reveal that the g factors for the high-spin states can provide important quantitative signatures vis-à-vis the occurrence of various structural changes in the anomalous yrast spectra in the germanium region.

I. INTRODUCTION

A convenient probe to test the predictions of various nuclear models is provided by the interactions of nuclei with the electromagnetic field.¹ In this context, a measurement of the gyromagnetic factors of nuclear levels is expected to furnish sensitive structural information primarily because of the large difference between the orbital and spin components of the single-particle magnetic moments of the active protons and neutrons.

A number of experimental studies²⁻⁶ have in the past provided valuable information concerning the g factors of the yrast 2^+ states in some Ge and Se isotopes. The available data have been examined in the framework of some phenomenological models;⁷ these analyses have been useful in assessing the relative applicability of various types of collective models. However, the observed g factors have not been analyzed in a microscopic framework so far.

The structure of the nuclei in the Ge region is quite complex. This is mainly due to the fact that the shell-model orbits spanning the underlying configuration space do not exhibit strong subshell closures between the magic numbers 28 and 50 (Ref. 8). A realistic description of the yrast g factors in the Ge and Se isotopes is, therefore, expected to involve a reasonably large valence space outside the ^{56}Ni core. Apart from the near intractability of the conventional configuration-mixing shell-model calculations for these valence spaces, a microscopic description is also rendered difficult for want of precise quantitative estimates concerning the renormalization of the orbital and spin g factors for the valence protons and neutrons due to the ^{56}Ni core-excitation processes.

The purpose of this work is twofold. We first demonstrate that the available data involving the g factors of a number of yrast 2^+ states in the Ge region can be interpreted in a microscopic, parameter-free manner in the framework of the variation-after-projection (VAP) method⁹ in conjunction with the realistic effective in-

teractions operating in the $(2p_{3/2}, 2p_{1/2}, 1f_{5/2}, 1g_{9/2})$ space. The effects due to the excitations from the ^{56}Ni core are sought to be included via an explicit renormalization of the magnetic-moment operator associated with the valence nucleons in terms of various first- and second-order perturbative diagrams.¹⁰ We have examined in this context the efficacy of the empirical prescriptions that have often been employed in the past to characterize the effective magnetic-moment operator for valence nucleons in restricted configuration spaces. Second, we examine whether the $g(J^\pi)$ values for $2^+ \leq J^\pi \leq 12^+$ could also provide unambiguous signatures of the anomalous features observed in a number of recent experimental investigations⁸ of the high-spin yrast spectra in the Ge region.

In Sec. II we outline briefly the calculational framework. The results of the calculation of the g factors for the yrast levels in the nuclei $^{68,70,72,74,76}\text{Ge}$ and $^{72,74,76,78,80}\text{Se}$ are presented and discussed in Sec. III. Finally, Sec. IV contains some concluding remarks.

II. CALCULATIONAL FRAMEWORK

A. The yrast g factors in terms of the wave functions resulting from the VAP approach applied to the $(2p_{3/2}, 2p_{1/2}, 1f_{5/2}, 1g_{9/2})^{\pi,\nu}$ space

The wave functions for the yrast levels in the nuclei $^{68,70,72,74,76}\text{Ge}$ and $^{72,74,76,78,80}\text{Se}$ have been obtained by invoking the VAP prescription in conjunction with the Hartree-Fock-Bogoliubov (HFB) ansatz¹¹ for the intrinsic states. The VAP wave functions have earlier been successfully employed in the context of the microscopic description of the yrast levels and the electromagnetic transition probabilities in the Ge region.⁹ However, their use in the calculation of the yrast g factors has not been reported thus far. In what follows we briefly sketch an outline of the VAP prescription as it applies to the calcu-

lation of the g factors of the yrast levels. The axially symmetric HFB state can be written as

$$|\Phi_0\rangle = \Pi_{im} (U_{im} + V_{im} b_{im}^\dagger b_{i\bar{m}}^\dagger) |0\rangle, \quad (1)$$

where the creation operators b_{im}^\dagger can be expressed as

$$\begin{aligned} b_{im}^\dagger &= \sum_j c_{im}^j a_{jm}^\dagger, \\ b_{i\bar{m}}^\dagger &= \sum_j (-1)^{l+j-m} c_{im}^j a_{j\bar{m}}^\dagger. \end{aligned} \quad (2)$$

Here the creation operators a_{jm}^\dagger creates a particle in the orbit $|nljm\rangle$ and c_{im}^j are the expansion coefficients. The index j labels the single-particle states $2p_{3/2}$, $2p_{1/2}$, $1f_{5/2}$, and $1g_{9/2}$, and the index i is employed to distinguish between different deformed single-particle states with the same m .

The states with good angular momenta projected from the HFB state $|\Phi_K\rangle$ can be written as

$$\begin{aligned} |\Psi_{M(K)}^J\rangle &= P_{MK}^J |\Phi_K\rangle \\ &= [(2J+1)/8\pi^2] \int D_{MK}^J(\Omega) R(\Omega) |\Phi_K\rangle d\Omega, \end{aligned} \quad (3)$$

where $R(\Omega)$ and $D_{MK}^J(\Omega)$ are the rotation operator and the rotation matrix, respectively.

$$g(J^\pi) = \langle \Psi_{0(0)}^J | \hat{\mu}_z | \Psi_{0(0)}^J \rangle / J$$

$$= (n^J J)^{-1} \int_0^{\pi/2} n(\theta) \sum_m \begin{bmatrix} J & 1 & J \\ -m & m & 0 \end{bmatrix} d_{-m0}^J(\theta) \left[\sum_{\tau_3 \alpha \beta} \langle \alpha | \hat{\mu}_m | \beta \rangle_{\tau_3} \left[\frac{M(\theta)}{1+M(\theta)} \right]_{\alpha\beta}^{\tau_3} \right] \sin\theta d\theta. \quad (7)$$

Here the term in square brackets is a Clebsch-Gordan coefficient. The explicit expressions for the normalizations n^J and the matrices $n(\theta)$ and $M(\theta)$ have been given in Ref. 9.

In our VAP calculations of the yrast wave functions we treat the doubly closed nucleus ^{56}Ni as an inert core. The relevant effective two-body interaction that we have employed is a renormalized G matrix due to Kuo.¹² In addition to providing a satisfactory explanation¹³ of the observed anomalous sequence of the high-spin yrast spectra in ^{60}Ni in the exact shell-model framework, this interaction has also recently described successfully the $B(E2, 0^+ \rightarrow 2^+)$ systematics^{9,14} and the yrast spectra⁹ in the set of Ge and Se isotopes considered here. The single-particle energies we have taken are (in MeV): $\epsilon(2p_{3/2})=0.00$, $\epsilon(1f_{5/2})=0.78$, $\epsilon(2p_{1/2})=1.08$, and $\epsilon(1g_{9/2})=3.50$ for the Ge isotopes. In our calculations for the Se isotopes we take $\epsilon(1g_{9/2})=3.25$.

B. The renormalization of the magnetic dipole moment operator associated with the model-space protons and neutrons due to the $1f_{7/2}$ core-excitation processes

The magnetic dipole moment operator appearing in Eq. (7) is an *effective* single-particle operator associated

The energy of the state with the angular momentum J is given as

$$E_J = \langle \Phi_0 | HP_{00}^J | \Phi_0 \rangle / \langle \Phi_0 | P_{00}^J | \Phi_0 \rangle, \quad (4)$$

where H is the shell-model Hamiltonian given by

$$H = \sum_\alpha \epsilon(\alpha) a_\alpha^\dagger a_\alpha + \frac{1}{4} \sum_{\alpha\beta\gamma\delta} \langle \alpha\beta | V | \gamma\delta \rangle a_\alpha^\dagger a_\beta^\dagger a_\delta a_\gamma. \quad (5)$$

Here α denotes the set of quantum numbers $(n_\alpha, l_\alpha, j_\alpha, m_\alpha)$.

The VAP procedure involves the selection of an appropriate intrinsic state for *each* yrast level through a minimization of the expectation value of the Hamiltonian with respect to the states of good angular momentum given by Eq. (3). One first generates the self-consistent intrinsic states $\Phi(\beta)$ by carrying out the HFB calculation with the Hamiltonian $(H - \beta Q_0^2)$. The *optimum* intrinsic state for *each* yrast level, $\Phi_{\text{opt}}(\beta_J)$, is then selected by ensuring that the following condition be satisfied:

$$\delta[\langle \Phi(\beta) | HP_{00}^J | \Phi(\beta) \rangle / \langle \Phi(\beta) | P_{00}^J | \Phi(\beta) \rangle] = 0. \quad (6)$$

Using the angular momentum projected wave functions $|\Psi_{M(K)}^J\rangle$ resulting from the optimum intrinsic states one obtains the following expression for the g factors of the yrast states:

with the extra-core (or valence) nucleons that is expected to *simulate* the effects due to the ^{56}Ni core excitations. This operator can be described by the general expression¹

$$\hat{\mu}_{\text{eff}} = g'_l l + g'_s s + g_p (Y^{(2)} \times s^{(1)})^{(1)}, \quad (8)$$

where g'_l (g'_s) are the effective orbital (spin) g factors and g_p provides a measure of the spin-polarization effects. The use of the G matrix calculated by Kuo is expected to provide a compensation for the *additional* configuration mixing *within* the $(2p_{3/2}, 2p_{1/2}, 1f_{5/2}, 1g_{9/2})^n$ space that is expected to result from a consideration of the extended valence space involving the $1f_{7/2}$ orbit. On the other hand, the use of these effective g factors¹⁵ is intended to simulate, at least partially, the effects due to an *explicit* inclusion of the configurations such as

$$[(1f_{7/2})^{-m} (2p_{3/2}, 2p_{1/2}, 1f_{5/2}, 1g_{9/2})^{n+m}].$$

In the present work we have first obtained the first- as well as second-order renormalization of the diagonal matrix elements $\langle j_{\frac{1}{2}} | \mu | j_{\frac{1}{2}} \rangle^{\pi, \nu}$ ($j = \frac{1}{2}, \frac{3}{2}, \frac{5}{2}$). These renormalized matrix elements were next transcribed, via Eq. (8), into a *unique* set of six parameters $(g'_l, g'_s, g_p)^{\pi, \nu}$. The first-order renormalization of the reduced matrix ele-

ments $\langle j || \mu || j \rangle$, for example, is obtained by evaluating Fig. 1(a):

$$\begin{aligned} \langle\langle j || \hat{\mu} || j \rangle\rangle &= \langle j || \hat{\mu} || j \rangle - 2 \sum_{j_p, J} (\epsilon_{j_h} - \epsilon_{j_p})^{-1} \langle j_h || \mu || j_p \rangle \\ &\quad \times (-1)^{j+j_p-J} W(jj_p jj_h, J1) \\ &\quad \times \langle jj_p | V | jj_h \rangle_J. \end{aligned} \quad (9)$$

Here the isotopic spin labels have been suppressed. The explicit expressions for the contributions arising from the second-order diagrams 1(b), 1(c), and 1(d) shown in Fig. 1 have been given in Ref. 10.

The effective interaction involved in the perturbative renormalization of the (diagonal) matrix elements of $\hat{\mu}$ is a slightly modified version¹⁶ of the Kuo-Brown interaction.¹⁷ Apart from reproducing correctly the deformation systematics in the $2p-1f$ shell, this interaction has also provided a successful description¹⁸ of the observed suppression of the $M1$ and $M3$ magnetic moments as well as form factors in the nucleus ^{57}Ni in terms of various first- and second-order graphs. The perturbative approach for obtaining the renormalized magnetic dipole moment operator derives its validity from the fact that the minimum-energy spherical HF solution for the nucleus ^{56}Ni resulting from this interaction is characterized by an energy gap of about 6.8 MeV between the occupied $1f_{7/2}$ orbit and the unoccupied orbits, setting thereby reasonable lower limits on the energy denominators involved in the expressions for various first- as well as second-order diagrams.

In Table I we have presented the contributions to the g'_i , g'_s , and g_p values due to various first- and second-order ^{56}Ni core-excitation processes displayed in Fig. 1. A large part of the renormalization of the g_s^π and g_s^v values arises from just the first-order diagrams. An in-

teresting feature of the second-order results given here is the partial cancellation of the dequenching due to the Tamm-Dancoff (or the RPA) graphs 1(c) by the contributions arising from the renormalization graphs 1(d). Further, it is seen that the spin-polarization term appearing in Eq. (8) owes its origin as much to the second-order diagrams as to the first-order ones. It turns out that the *total* first- as well as second-order renormalization of the matrix elements of $\hat{\mu}$ in the configuration space $(2p_{3/2}, 2p_{1/2}, 1f_{5/2}, 1g_{9/2})^{\pi, v}$ yields the following values for the parameters characterizing the effective (single-particle) magnetic moment operator for the valence protons and neutrons:

$$\begin{aligned} (g'_i, g'_s, g_p)^\pi &= (0.89, 3.18, 0.73), \\ (g'_i, g'_s, g_p)^v &= (0.07, -1.52, -0.89). \end{aligned}$$

III. RESULTS AND DISCUSSION

In Fig. 2 we have presented the observed as well as the theoretical estimates for the g factors of the states with $2^+ \leq J^\pi \leq 12^+$ resulting from the VAP prescription in conjunction with the renormalized $(g'_i, g'_s, g_p)^{\pi, v}$ values discussed in the preceding section. We have also presented here the VAP predictions resulting from various empirical choices of the parameters $(g_s^{\pi, v})$, as well as the estimates obtained in the framework of the projected HFB technique; the latter have been shown only for the renormalized values of the single-particle g factors.

We first discuss here the $g(2^+)$ predictions resulting from the VAP framework and the renormalized magnetic dipole moment operator given by Eq. (8). One finds that the estimates obtained in the present parameter-free framework are consistent with the available data for the yrast 2^+ states. In particular, they support the reevaluat-

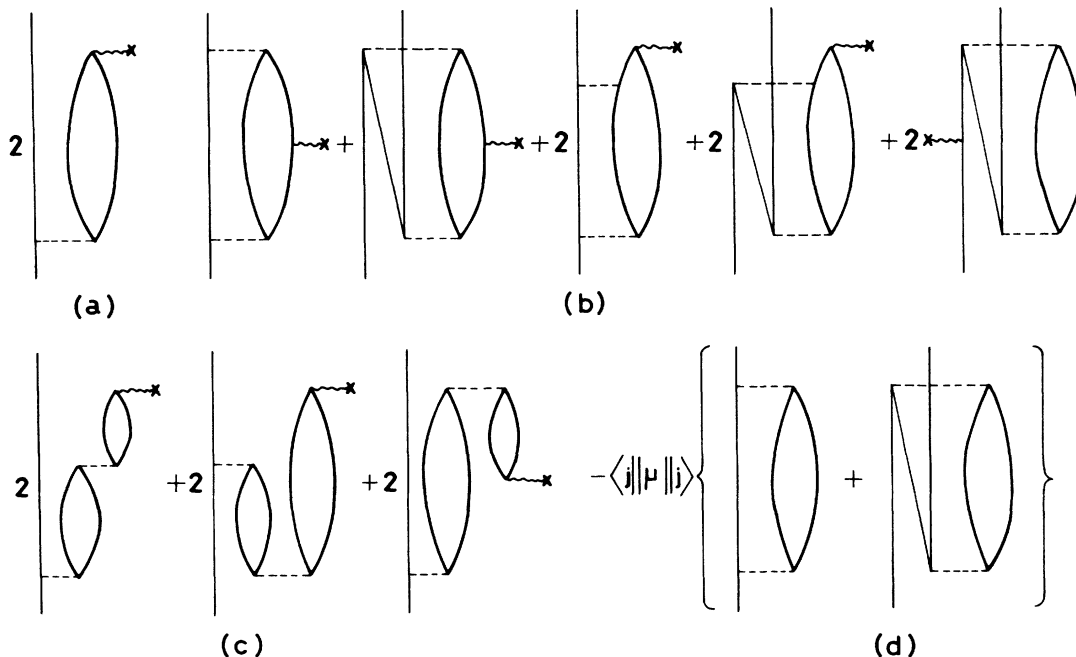


FIG. 1. Various first- and second-order diagrams contributing to the renormalization of the magnetic-moment operator associated with the valence protons and neutrons.

TABLE I. First- and second-order contributions (in units of the nuclear magneton) to the effective g factors [see Eq. (8)] for valence nucleons arising from various core-excitation processes displayed in Fig. 1. The corrections due to the Tamm-Dancoff and RPA graphs [Figs. 1(c)] as well as those due to the core-renormalization graphs [Figs. 1(d)] have been given separately. The zeroth-order values of the g factors are $[(g_1, g_s, g_p)^\pi, (g_1, g_s, g_p)^\nu] = [(1.00, 5.58, 0.00), (0.00, -3.82, 0.00)]$.

	Δg_l^π	Δg_s^π	Δg_p^π	Δg_l^ν	Δg_s^ν	Δg_p^ν
First-order diagrams 1(a)	0.034	-2.739	0.448	-0.024	2.471	-0.557
Second-order diagrams 1(b)	0.061	-0.043	0.355	-0.039	0.449	-0.121
Second-order diagrams 1(c)	-0.020	1.551	-0.217	0.013	-1.586	0.499
Second-order diagrams 1(d)	-0.186	-1.166	0.147	0.119	0.967	-0.712
Total contribution [diagrams 1(a)-1(d)]	-0.112	-2.397	0.733	0.069	2.301	-0.891

ed version⁴ of the experimental results in the Ge isotopes obtained earlier by Hubler *et al.*³ Considering next the $g(J^\pi)$ values for the higher yrast states with $J^\pi > 2^+$, one finds that in a number of cases the VAP predictions are characterized by significant J dependence. It is interesting to note in this context that the VAP results for the

yrast 2^+ states are quite close to the J independent predictions⁷ based on the collective model; the latter, in fact, provide a significant touchstone for comparison. The variations in the calculated $g(J^\pi)$ values for the yrast cascade are particularly striking in the case of the nuclei ^{72,74}Se and ^{68,70}Ge; in fact the $g(8^+)$ values in the latter isotopes are only about 50% of the $g(2^+)$ values. As we discuss later in the paper, this dramatic reduction in the yrast g factors is closely related to the increased participation of the neutrons (vis-à-vis the total angular momentum of the yrast state) that is triggered by the enhanced intrinsic deformation of these nuclei at higher spins.

A number of calculations^{19,20} have recently been carried out in the rare-earth region with a view to examining the structural changes associated with the backbending phenomenon in terms of the variation of the $g(J^\pi)$ values. In these calculations the renormalization of the magnetic-moment operator due to core excitations has been invoked by employing the parameters g'_s which are just 60% of the bare ones. We have tried to assess here the validity of this prescription²¹ in the context of the VAP wave functions in the Ge region. In Fig. 2 we have displayed the $g(J^\pi)$ estimates calculated with the values $(g_l^\pi, g_l^\nu) = (1.0, 0.0)$ for the orbital g factors and the values $0.6(g_s)_{\text{bare}}^{\pi, \nu}$ for the spin g factors. Although the qualitative features of the $g(J^\pi)$ vs J plots are not changed, our results indicate that the prescription employed in the earlier work is not particularly efficacious *quantitatively*. In the nuclei ^{68,70}Ge and ^{72,74}Se, for example, one can account for only about 50% of the actual renormalization of the yrast magnetic moments if one employs the empirical g_s factors.

In view of the increased sensitivity of the VAP magnetic-moment predictions for the higher members of the yrast bands towards various choices of the effective single-particle g factors associated with the valence nucleons, a reasonably accurate measurement of the magnetic moments of these states would not only be interesting in itself, it would also provide important quantitative information regarding the magnitude of various components of the renormalized magnetic-moment operator for the valence space involved in the present microscopic description.

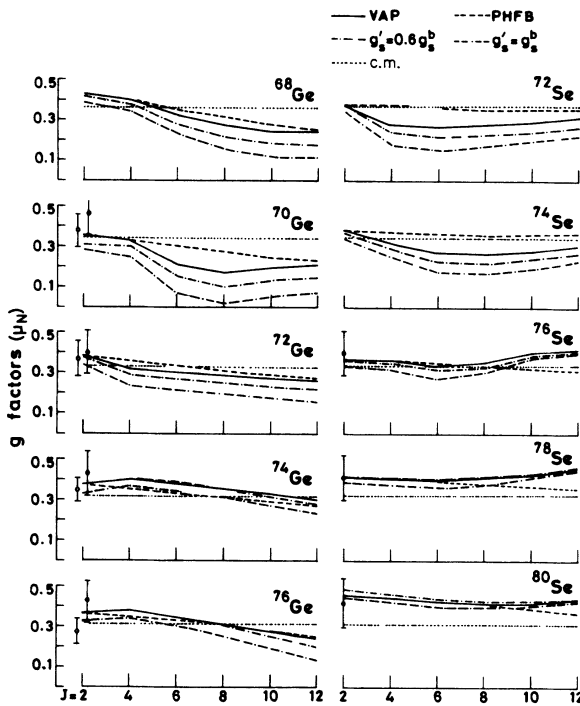


FIG. 2. The g factors of the yrast states in the nuclei ^{68,70,72,74,76}Ge and ^{72,74,76,78,80}Se. The solid (dashed) line shows the VAP (PHFB) estimates obtained by using the renormalized values of the parameters characterizing the magnetic-moment operator for valence nucleons. The VAP g factors resulting from the prescription discussed in Ref. 20, as well as the estimates involving the use of the unrenormalized valence μ operator have been shown by the dash-dotted and the double dash-dotted curves, respectively. The dotted line represents the J -independent predictions resulting from the phenomenological collective models (Ref. 7). The data for Ge isotopes are taken from Ref. 6 (closed circles) and Ref. 4 (open circles). The data for Se isotopes have been taken from Ref. 2 (closed circles).

TABLE II. The quadrupole deformations $\langle \Phi_{\text{opt}}(\beta_J) | Q_0^2 | \Phi_{\text{opt}}(\beta_J) \rangle$ of the optimum intrinsic states resulting from the VAP procedure in the nuclei $^{68,70,72,74,76}\text{Ge}$ and $^{72,74,76,78,80}\text{Se}$. The expectation values of the operators Q_0^2 and J^2 for the HFB intrinsic states have also been given. The intrinsic quadrupole moments have been given in units of b^2 , where $b (= \sqrt{\hbar/m\omega})$ is the oscillator constant.

Nucleus	$J_{\text{yrast}} = 2^+$	$\langle \Phi_{\text{opt}}(\beta_J) Q_0^2 \Phi_{\text{opt}}(\beta_J) \rangle$					$\langle Q_0^2 \rangle_{\text{HFB}}$	$\langle J^2 \rangle_{\text{HFB}}$
		4^+	6^+	8^+	10^+	12^+		
^{68}Ge	28.4	28.4	30.6	31.7	32.0	32.6	28.4	14.5
^{70}Ge	32.1	32.1	35.6	37.2	37.5	37.5	32.1	23.6
^{72}Ge	31.0	33.2	33.2	33.2	33.2	33.2	31.0	20.5
^{74}Ge	30.1	28.0	26.9	26.9	26.9	26.9	30.1	20.1
^{76}Ge	26.5	26.5	26.5	26.5	26.5	26.5	27.6	18.9
^{72}Se	35.9	39.4	39.4	40.8	40.8	40.8	35.9	26.9
^{74}Se	36.4	38.6	40.5	41.6	41.6	41.7	36.4	26.2
^{76}Se	35.5	35.5	36.3	37.3	37.7	38.1	35.5	27.8
^{78}Se	32.2	32.2	32.2	33.3	33.3	33.3	32.2	25.6
^{80}Se	27.2	27.2	28.1	28.1	28.1	28.1	27.2	20.5

In order to bring out the specific role of the VAP degree of freedom vis-à-vis the J dependence of the calculated results, we have also presented here the predictions resulting from the usual projected HFB method involving *single* intrinsic wave function for *all* the yrast states. It is seen that the VAP predictions differ significantly from the projected Hartree-Fock-Bogoliubov (PHFB) ones in the range $4^+ \leq J^\pi \leq 10^+$ in the lighter Ge and Se isotopes. The VAP estimates for the $g(6^+)$ and $g(8^+)$ values in ^{70}Ge , for example, are only about 60% of the corresponding PHFB results. These results are not entirely unanticipated in view of the significant variation of the quadrupole deformations of the relevant optimum intrinsic states along the yrast cascade (see Table II). A striking feature of the projected HFB results is the nearly *linear* decrease of the $g(J^\pi)$ values. Further, one observes that the slope of the $g(J^\pi)$ vs J plots is roughly proportional to the $\langle \hat{J}^2 \rangle^{-1}$ values; in fact the $[g(J^\pi)]_{\text{PHFB}}$ values can easily be parametrized in terms of the relation $g(J^\pi) = [g(2^+) + \alpha(J-2)/\langle \hat{J}^2 \rangle^{-1}]$, involving nearly mass-independent parameter α . Thus, the near constancy (as a function of J) of the $g(J^\pi)$ values in the Se isotopes is simply due to the enhanced values of $\langle \hat{J}^2 \rangle$ (see Table II). The PHFB results presented here seem to provide an interesting illustration of the validity of the systematic approximation procedure, suggested some time ago by Villars,²² which is based on an expansion of the projected HF/HFB expectation values in terms of $[\langle \hat{J}^2 \rangle]^{-1}$.

In what follows we discuss the mechanism underlying the dramatic changes in the calculated $g(J^\pi)$ values for $J^\pi = 6^+, 8^+$ that are observed in some cases considered here. As seen from the results presented in Table II, the quadrupole deformations of the optimum intrinsic states associated with the yrast levels in the nuclei $^{68,70}\text{Ge}$ and $^{72,74}\text{Se}$ display considerable variation between $J^\pi = 2^+$ and $J^\pi = 12^+$. For example, the value of $\langle \Phi_{\text{opt}}(\beta_J) | Q^2 | \Phi_{\text{opt}}(\beta_J) \rangle$ changes by as much as 15% in going from the level 2^+ to the level 12^+ in the case of the nucleus ^{68}Ge . An efficient mechanism for increasing the deformation of an intrinsic state (associated with a yrast level) is to promote *neutrons* from the occupied deformed orbitals of the $(2p_{3/2}, 1f_{5/2})$ parentage to the orbitals

$1g_{9/2, \pm 1/2}$; the excitation of protons is *not* favored energetically in this context. An essential implication of this process is the increased involvement of the neutrons vis-à-vis the total angular momentum of the state. This is illustrated by the results for the ^{70}Ge yrast states presented in Table III; the results obtained in the case of the yrast states for other nuclei are similar. We have given here the individual contributions of the expectation values of the operators \hat{I}_z , \hat{s}_z , and $(Y^{(2)}_s)^{(1)}_z$ with respect to the yrast wave functions—this way of presenting the yrast g factor results brings out their *explicit dependence* on the parameters characterizing the magnetic dipole moment operator for valence nucleons. It is seen that the relative contribution of the neutrons towards the total angular momentum of the state registers a sharp increase for the higher members of the yrast band; whereas the expectation value $\langle \hat{J}_z \rangle^\nu (= \langle \hat{I}_z \rangle^\nu + \langle \hat{s}_z \rangle^\nu)$ accounts for only about 60% of the total angular momentum for the $J^\pi = 2^+$ state, its share increases to about 80% in the $J^\pi = 8^+$ state. An increased neutron contribution towards the total angular momentum implies a suppression of the $\langle \hat{J}_z \rangle^\pi$ values. This results in a significant reduction in the $g(J^\pi)$ values which are quantitatively quite sensitive towards the proton contributions because of the large values of the effective g_l^π factors associated with valence protons—the latter are an order of magnitude larger than the relevant effective g_l^ν factors.

As shown in the results presented in Table III, one finds that the polarization term involving the operator $(Y^{(2)}_s)^{(1)}_z$ yields consistently small contributions for protons as well as neutrons. This feature is not very surprising since a large magnitude of the matrix element $\langle (Y^{(2)}_s)^{(1)}_z \rangle$ —and this can be approximated to a good extent by the product of the matrix elements $\langle Y_z^{(2)} \rangle$ and $\langle \hat{s}_z \rangle$ —is difficult due to somewhat conflicting requirements for obtaining large matrix elements separately for the operators $Y^{(2)}$ and $s^{(1)}$; whereas the former requires half-filled shells with $j = l \pm \frac{1}{2}$, the latter is maximized when the full occupation of just one of the two spin-orbit partners is realized.

The general form of the magnetic moment operator [see Eq. (8)] permits a discussion of the VAP results for

TABLE III. The g factors (in units of the nuclear magneton) for the yrast levels (with $J^\pi = 2^+ - 12^+$) in the nucleus ^{70}Ge . We have presented in columns 2–7 the contributions arising from the protons and neutrons towards the expectation values of the operators l_z , s_z , and $(Y_s^{(2)})_z^{(1)}$. The theoretical estimates for the yrast g factors resulting from the bare as well as the renormalized values of the parameters $g_l^{\pi,\nu}$, $g_s^{\pi,\nu}$, and $g_p^{\pi,\nu}$ (see text) have been labeled $g(J_{\text{bare}}^\pi)$ and $g(J_{\text{ren}}^\pi)$, respectively.

J^π	$\langle l_z \rangle$	Protons $\langle s_z \rangle$	$\langle (Y_s)_z^1 \rangle$	$\langle l_z \rangle$	Neutrons $\langle s_z \rangle$	$\langle (Y_s)_z^1 \rangle$	$g(J_{\text{bare}}^\pi)$	$g(J_{\text{ren}}^\pi)$	$g(J_{\text{expt}}^\pi)$
2^+	0.80	-0.001	-0.034	1.14	0.059	-0.030	0.284	0.353	0.38 ± 0.08^a 0.47 ± 0.10^b 0.47 ± 0.12^c
4^+	1.52	-0.004	-0.064	2.35	0.131	-0.057	0.249	0.330	
6^+	1.64	-0.008	-0.067	4.07	0.298	-0.058	0.075	0.214	
8^+	1.86	-0.002	-0.066	5.68	0.457	-0.047	0.014	0.172	
10^+	2.51	0.019	-0.077	6.92	0.553	-0.056	0.050	0.196	
12^+	3.13	0.042	-0.087	8.17	0.658	-0.064	0.071	0.210	

^aReference 4.

^bReference 4. These values represent the reevaluated version of the data reported earlier by G. K. Hubler *et al.* (Ref. 3).

^cReference 6.

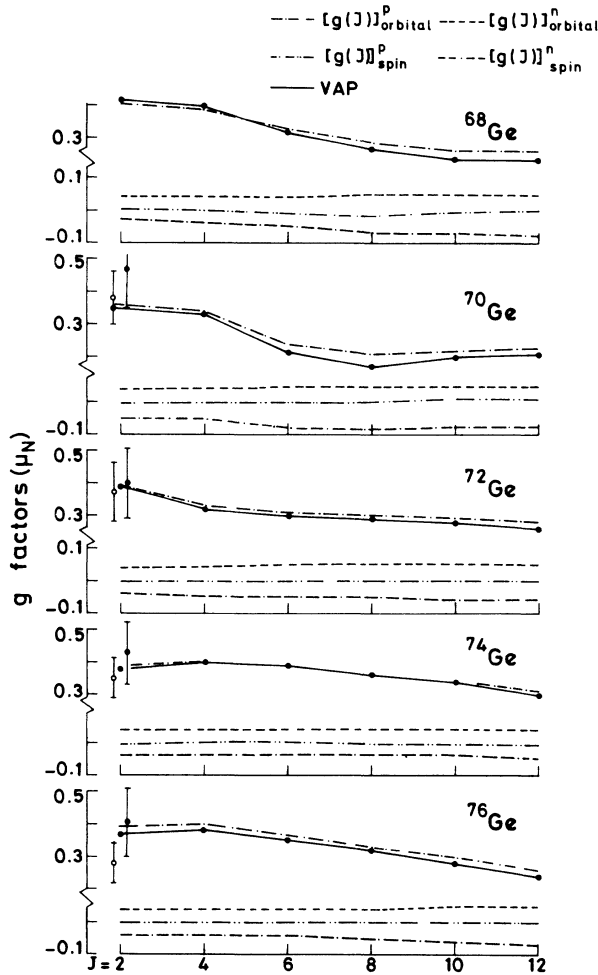


FIG. 3. The contributions to the yrast g factors in the Ge isotopes resulting from the orbital and spin components associated with the magnetic-moment operator for the valence protons and neutrons. These results have been labeled $[g(J)]_{\text{orbital/spin}}^{p/n}$.

the yrast $g(J^\pi)$ values—in particular their J dependence—in terms of their orbital and spin components associated with the valence protons and neutrons. In Figs. 3 and 4 we have displayed the individual contributions if the terms $g_l^{\pi(\nu)} \langle \hat{l}_z \rangle^{\pi(\nu)}$ and $g_s^{\pi(\nu)} \langle \hat{s}_z \rangle^{\pi(\nu)}$ (hereafter referred to as $[g(J^\pi)]_{\text{orbital}}^{p(n)}$ and $[g(J^\pi)]_{\text{spin}}^{p(n)}$, respectively) for the yrast levels in various Ge and Se isotopes. These results reveal the following features.

(1) Considering first the yrast states with $J^\pi = (2^+, 4^+, 6^+)$, one finds that the calculated VAP re-

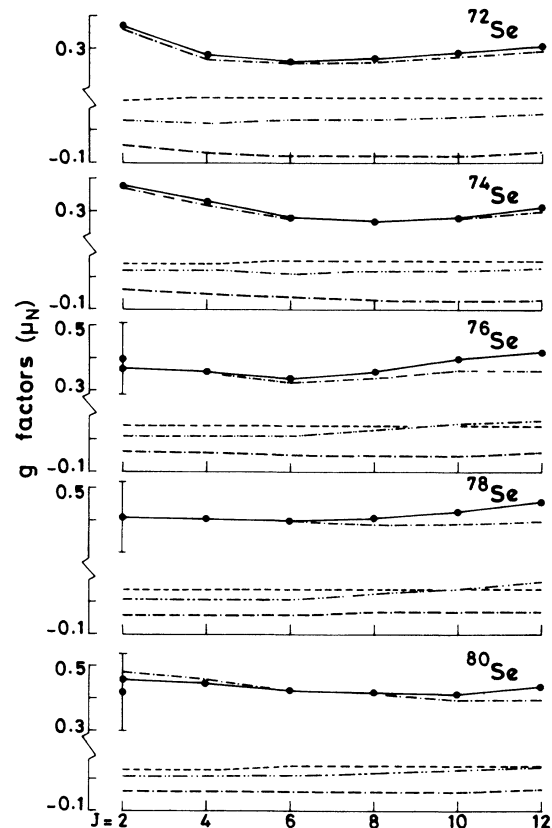


FIG. 4. The results obtained in the case of the Se isotopes.

sults are dominated by the $[g(J^\pi)]_{\text{orbital}}^p$ contributions in the nuclei considered here. This feature is due to the smallness of the spin contributions of the valence protons as well as the near cancellation of the spin and orbital contributions of the valence neutrons for these states.

(2) Considering next the higher part of the yrast spectrum (with $J^\pi = 8^+, 10^+, 12^+$) one notes that, whereas the spin contributions arising from the valence neutrons become important in the nuclei $^{68,70}\text{Ge}$, the spin contributions due to valence protons acquire quantitative significance in the nuclei $^{76,78,80}\text{Se}$. An examination of the structure of the relevant optimum intrinsic states associated with these yrast levels reveals that the conspicuous increase in the $\langle s_z \rangle^{\nu, \pi}$ contributions arises due to an increased involvement of the $(1g_{9/2})^\nu$ orbit in the lighter Ge isotopes and the $(1g_{9/2})^\pi$ orbit in the heavier Se isotopes. As seen from the results presented in Table III, the $\langle s_z \rangle^\nu$ contribution increases significantly—from 0.06 for the level $J^\pi = 2^+$ to 0.46 for the level $J^\pi = 8^+$ —in the nucleus ^{70}Ge . This is correlated with the changes in the $(1g_{9/2})^\nu$ subshell occupation numbers; the latter increase from 3.5 to 4.0 in this part of the yrast spectrum.

An important ramification of the enhanced effectiveness of the spin contributions vis-à-vis the high-spin states is the increased sensitivity of the calculated results towards the choices of the $(g_s')^{\pi, \nu}$ parameters. An interesting example in this context is provided by the ^{70}Ge results presented earlier in Fig. 2; here the use of the unrenormalized $(g_s')^\nu$ values is seen to yield vanishingly small VAP estimates for $g(8^+)$ since the increased (negative) value of the product $[(g_s')_{\text{bare}}^\nu \langle s_z \rangle^\nu]$ almost offsets quantitatively the contribution arising from the valence protons.

IV. CONCLUSIONS

We have discussed here the calculation of the g factors of the yrast states (with $2^+ \leq J^\pi \leq 12^+$) in some doubly even Ge and Se isotopes in the framework of the VAP prescription in conjunction with the renormalized magnetic dipole moment operator for the valence protons and neutrons in the $(2p_{3/2}, 1f_{5/2}, 2p_{1/2}, 1g_{9/2})^{\pi, \nu}$ space. Apart from providing a parameter-free microscopic description of the available $g(2^+)$ values, the results presented here have brought out the sensitivity of the yrast g factors towards specific structural features of the valence wave functions. The calculations have also emphasized the quantitative significance of the core-polarization effects (embodied in the effective orbital and spin g factors associated with the valence nucleons) vis-à-vis the variation of the $g(J^\pi)$ values along the yrast cascade. In this context, present study has illustrated the range within which different empirical choices of the single-nucleon g factors can alter the theoretical predictions. Our calculations underline the importance of the yrast g factor measurements for $J^\pi > 2^+$; in addition to allowing a rigorous and detailed critique of the ingredients of the microscopic framework presented here, these studies are expected to augment in an important manner our knowledge concerning the relative significance of various factors characterizing the anomalous yrast spectra in the Ge region.

One of us (P.K.R.) would like to thank the Council of Scientific and Industrial Research, India, for providing financial assistance.

*Permanent address: Department of Physics, Indian Institute of Technology Kanpur, Kanpur-20 80 16, India.

¹A. Bohr and B. R. Mottelson, *Nuclear Structure* (Benjamin, New York, 1969), Vol. 1, p. 336.

²G. M. Heestand *et al.*, Nucl. Phys. **A113**, 310 (1969).

³G. K. Hubler, H. W. Kugel, and D. E. Murnick, Phys. Rev. C **9**, 1954 (1974).

⁴C. Fahlander, K. Johansson, E. Karlsson, and G. Possnert, Nucl. Phys. **A291**, 241 (1977).

⁵B. Singh and D. A. Viggars, Nucl. Data Sheets **42**, 233 (1984).

⁶A. Pakaou *et al.*, J. Phys. G **10**, 1759 (1984).

⁷W. Greiner, Nucl. Phys. **60**, 417 (1966).

⁸M. Vergnes, in *Proceedings of the Conference on the Structure of Medium-Heavy Nuclei, Rhodes, 1979*, edited by the Demokritos Tandem Accelerator Group, Athens (IOP, Bristol, 1980), p. 80.

⁹P. N. Tripathi and S. K. Sharma, Phys. Rev. C **34**, 1081 (1986).

¹⁰B. Ghosh and S. K. Sharma, Phys. Rev. C **29**, 648 (1984).

¹¹A. L. Goodman, in *Advances in Nuclear Physics*, edited by J. W. Negele and E. Vogt (Plenum, New York, 1979), Vol. 11.

¹²T. S. Kuo (private communication).

¹³V. Potbhare, S. K. Sharma, and S. P. Pandya, Phys. Rev. C **24**, 2355 (1981).

¹⁴D. P. Ahalpara and K. H. Bhatt, Phys. Rev. C **25**, 2072 (1982).

¹⁵P. W. M. Glaudemans, *Proceedings of the Conference on the Structure of Medium-Heavy Nuclei, Rhodes, 1979*, Ref. 8, p. 11.

¹⁶J. B. McGrory, B. H. Wildenthal, and E. C. Halbert, Phys. Rev. C **2**, 186 (1970).

¹⁷T. S. Kuo and G. E. Brown, Nucl. Phys. **A114**, 241 (1968).

¹⁸B. Ghosh and S. K. Sharma, Phys. Rev. C **32**, 643 (1985).

¹⁹M. Diebel, A. N. Mantri, and U. Mosel, Nucl. Phys. **A345**, 72 (1980); A. N. Mantri, M. Diebel, and U. Mosel, Phys. Rev. Lett. **47**, 308 (1981).

²⁰A. Ansari, E. Wüst, and K. Mühlhans, Nucl. Phys. **A415**, 215 (1984).

²¹D. Schwalm, Nucl. Phys. **A396**, 339C (1983).

²²F. Villars, in *Many-Body Description of Nuclear Structure Reactions*, Proceedings of the International School of Physics "Enrico Fermi," Course 36, Varenna, edited by C. Bloch (Academic, New York, 1966).